Quark Confinement from different Dressed Gluon Propagators

Marco A. Bedolla (marco.bedolla@unach.mx)
Universidad Autónoma de Chiapas
Khépani Raya
Universidad de Huelva
Alfredo Raya
Universidad Michoacana de San Nicolás de Hidalgo

Research Article

Keywords: Schwinger-Dyson Equations, Gluon Propagator, Mass Function, Quark Mass

Posted Date: April 19th, 2023

DOI: https://doi.org/10.21203/rs.3.rs-2819694/v1

Additional Declarations: No competing interests reported.

Quark Confinement from different Dressed Gluon Propagators

Marco A. Bedolla[1*], Khépani Raya[2†] and Alfredo Raya[3,4†]

[1*]Facultad de Ciencias en Física y Matemáticas (FCFM), Universidad Autónoma de Chiapas, Carretera Zapata Km. 8, Rancho San Francisco, Tuxtla Gutiérrez, 29050, Chiapas, México.

[2]Dpto. Ciencias Integradas, Centro de Estudios Avanzados en Fis., Mat. y Comp., Fac. Ciencias Experimentales, Universidad de Huelva, Huelva, 21071, Spain.

[3]Instituto de Física y Matemáticas, Universidad Michoacana de San Nicolás de Hidalgo, Edificio C-3, Ciudad Universitaria. Francisco J. Mújica s/n, Col. Felícitas del Río,, Morelia, 58040, Michoacán, México.

[4]Centro de Ciencias Exactas, Universidad del Bio-Bio Avda. Andrés Bello 720, Casilla 447, Chillán, Chile.

*Corresponding author(s). E-mail(s): marco.bedolla@unach.mx;
Contributing authors: khepani.raya@dci.uhu.es; alfredo.raya@umich.mx;
†These authors contributed equally to this work.

Abstract

The gap equation in quantum chromodynamics is solved by incorporating different gluon dressing functions, some of them derived from a quark-diquark potential that exhibits a conformal symmetry. By using the bare vertex and working in the Landau gauge, the quark mass function is found to have an infrared enhancement that smoothly transitions to an asymptotically free behavior at high momentum, which is consistent with the predictions of Schwinger-Dyson equations. Additionally, these quark propagators violate reflexion positivity, indicating that the gluon dressing provides clear evidence of quark confinement.

Keywords: Schwinger-Dyson Equations, Gluon Propagator, Mass Function, Quark Mass

1 Introduction

The study of the gluon propagator is important because it is a key ingredient in understanding the non-perturbative aspects of Quantum Chromodynamics (QCD), the theory that describes the strong interactions between quarks and gluons, which is one of the fundamental forces of nature [1]. The gluon is responsible for confining quarks into hadrons, and the gluon propagator plays a crucial role in determining the behavior of quarks at low energies, where perturbative methods are not applicable [2–14], . Additionally, the gluon propagator is closely related to the phenomenon of chiral symmetry breaking, which is responsible for the generation of mass in hadrons [15–17]. Therefore, understanding the analytic behavior of the gluon propagator is essential for a complete understanding of the strong interactions and for predicting the properties of hadrons.

A recent approach consists in studying the presence of a conformal symmetry in massless QCD which has been crucial in improving our comprehension of the quark-gluon interactions in the ultraviolet region, where it is applicable to the first order and has been frequently used in calculating hard exclusive pQCD sum-rules. The strong coupling's walking behavior towards a constant value in the infrared region has been experimentally observed [18], which implies the existence of a conformal window.

The importance of conformal symmetry in QCD is also suggested by the gauge-gravity duality, which was first introduced by Maldacena [19]. According to this duality, a conformal theory at the boundary of AdS_5 space can be related to non-zero temperature QCD. The AdS_5 boundary has various conformal geometries, one of which is the compactified Minkowski space $R \times S^3$. This geometry is well-suited for introducing temperature, which is associated with the inverse radius of S^3 [20, 21]. This radius is expected to be significantly larger than Λ_{QCD}.

In addition, the $R \times S^3$ geometry is a useful framework for exploring the potential conformal symmetry properties of hadrons. This is because a two-particle system that displays excitation patterns consistent with conformal symmetry (such as a $q\bar{q}-$pair) can be easily modeled in $R \times S^3$ as one particle moving freely on S^3 while carrying the reduced mass of the system.

In this way, the conformal symmetry patterns observed in high-energy unflavored mesons with masses greater than 1400 MeV were modeled in a study by Kirchbach et.al. [22]. However, the motion can be refined by allowing for perturbations of the free motion through potentials that maintain the degeneracy patterns. In the same article, it was argued that the free motion of a scalar particle on S^3, when perturbed by a cotangent interaction, is well-suited for describing the aforementioned meson spectra.

Furthermore, the tuning of the radius of S^3 in accordance with the spectra resulted in a temperature value that was reasonable and at least twice the value of Λ_{QCD}. The cotangent interaction, also known as the "curved Coulomb" potential, is unique to the compactified Minkowski spacetime. The idea is that motion on S^3 that is perturbed by a cotangent function of the second polar angle can be transformed into a Casimir invariant of an algebra with the same commutation relations as $so(4)$ [23]. However, the components of this algebra are no longer Hermitian, which is why they cannot be included in the generator set that produces the conformal group.

All of this has motivated the proposal of various models the dressed gluon propagator which can have important implications for the behavior of the quark propagator and the phenomena of confinement and chiral symmetry breaking in QCD. Some of these models include:

1. Sinc model: This model is based on a Fourier transform of the Rosen-Morse trigonometric potential used to describe a quark-diquark potential. It is finite in the infrared and falls as $1/q^2$ at large momentum [24].
2. Struve model: This model is similar to the Sinc model, but the instantaneous propagator is obtained from first projecting the hyperspherical motion on the equatorial disk, a plane 3D space, and then performing a standard 3D Fourier transform to momentum space [25–27].
3. Lattice-based models: This model are based on a lattice QCD inspired form for the gluon propagator, which is characterized by an enhancement in the infrared and a fall-off as $1/q^4$ at large momentum. As example we have the Maris-Tandy [28] and the Qin [29] models
4. Algebraic models: These models are based on algebraic constraints imposed on the gluon propagator, such as the requirement of conformal symmetry or the requirement of infrared finiteness [30, 31].

On the other hand, the use of Schwinger-Dyson Equation (SDE) approaches has been employed to study confinement and the dressing function of the gluon propagator in the conformal window regime. SDEs are a powerful tool for understanding hadronic physics, and significant progress has been made over the past two decades in describing hadron physics using this framework. SDEs can rival and complement predictions made by other non-perturbative approaches such as lattice QCD and constituent quark models. A number of reviews on this topic can be found in the literature [2–14], and these are summarized and extended in Ref. [15].

The framework of SDEs offers a viable explanation for how Dynamical Chiral Symmetry Breaking (DCSB) and Confinement, both emergent features of QCD, are related. In fact, it is believed that the former is a direct outcome of the latter. Furthermore, the increased quark mass function in the infrared is thought to arise from the gluon cloud that surrounds the quark at low momenta [32]. These phenomena can be investigated by examining the gap equation of QCD.

In this contribution, we investigate the relationship between DCSB and Confinement by using an effective model for the QCD gap equation. Our approach involves minimalistic assumptions where we use the bare vertex and a model of the gluon dressing function to examine the quark propagator in Landau gauge. The gluon dressing function we use is based on the instantaneous propagator of the curved Coulomb potential, along with some variations that capture the infrared and ultraviolet properties of the dressing function. We compare the predictions of relevant hadronic observables derived from our model with established phenomenological values, and we find that there are indications of compatibility between conformal and chiral dynamics for both low and high momentum regions of QCD. The remaining of this contribution is organized as follows: In Sect. 2, we review the generally accepted phenomenological aspects

of DCSB and Confinement from the gap equation. In Sect. 3 propose different effective gluon propagators and calculate and compare some relevant hadronic observables, which are afterward contrasted against well established predictions in Sect. 2. A brief summary and discussion our findings are provided in Sect. 4.

2 DCSB and Confinement: General aspects

We start from the Euclidean space [1] SDE for the quark propagator,

$$\begin{aligned} S(p)^{-1} &= Z_2(i\gamma\cdot p + m_b) \\ &+ Z_1\int^{\Lambda}\frac{d^4k}{(2\pi)^4}g^2 D_{\mu\nu}(q)\frac{\lambda^a}{2}\gamma_\mu S(k)\frac{\lambda^a}{2}\Gamma_\nu(k,p)\ , \end{aligned} \tag{1}$$

where $q = k - p$, λ^a represent the Gell-Mann matrices, m_b stands for the current-quark mass, g is the coupling constant, $D_{\mu\nu}(q)$ is the dressed gluon propagator and $\Gamma_\mu(k,p)$ is the full quark-gluon vertex. Moreover, Z_1 and Z_2 are, respectively, the vertex and quark wave function renormalization constants. The symbol $\int^{\Lambda}$ represents a regularization of the integrals at a scale Λ. The quark propagator, $S(p)$, has the general form

$$\begin{aligned} S(p) &= -i\gamma\cdot p\sigma_v(p^2) + \sigma_s(p^2) \\ &\equiv \frac{F(p^2)}{i\gamma\cdot p + M(p^2)}\ , \end{aligned} \tag{2}$$

such that the vector and scalar parts of the propagator, $\sigma_v(p^2)$ and $\sigma_s(p^2)$ are expressed in terms of the wave function renormalization $F(p^2)$ and the renormalization-point independent mass function $M(p^2)$ as

$$\sigma_v(p^2) = \frac{F(p^2)}{p^2 + M^2(p^2)}\ , \qquad \sigma_s(p^2) = \frac{F(p^2)M(p^2)}{p^2 + M^2(p^2)}\ . \tag{3}$$

The renormalized current quark mass

$$m = Z_4^{-1}Z_2 m_b, \tag{4}$$

where Z_4 is the renormalization constant of the Lagrangian quark mass, corresponds to the mass function at the renormalization scale. Therefore, the renormalization-group invariant current quark mass,

$$\hat{m} = \lim_{p^2\to\infty}\left[\frac{1}{2}\log\frac{p^2}{\Lambda}\right]^{\gamma_m} M(p^2)\ , \tag{5}$$

allows to take the chiral limit when $\hat{m} = 0$. Here, $\gamma_m = 12/(33 - 2N_f)$ is the mass anomalous dimension and Λ is identified with $\Lambda_{\rm QCD} = 0.234$ GeV. In all the above, we

[1] In our conventions, $\{\gamma_\mu, \gamma_\nu\} = 2\delta_{\mu\nu}$, $\gamma_\mu^\dagger = \gamma_\mu$, and $a\cdot b = \sum_{i=1}^4 a_i b_i$.

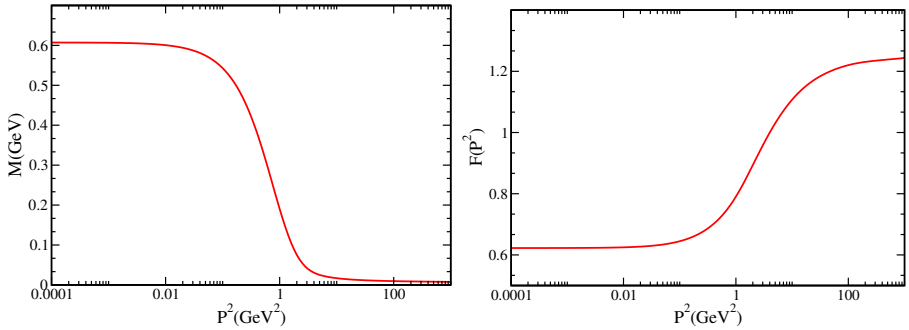

Fig. 1 Quark propagator for the MT model, Eq. (7). *Left panel:* Mass function. *Right panel:* Wave function renormalization. The renormalization scale is set to $\zeta = 2$ GeV and the quark bare mass is set to $m = 7$MeV.

have omitted the explicit dependence on the renormalization point ζ on the relevant quantities to avoid cumbersome notation.

A common practice to truncate the gap equation is to perform the replacement (Abelian approximation)

$$Z_1 g^2 D_{\mu\nu}(q)\Gamma_\mu(k,p) \to g^2_{\rm eff}\mathcal{G}(q^2)D^{\rm free}_{\mu\nu}(q)\gamma_\mu \ , \tag{6}$$

where $D^{\rm free}_{\mu\nu}(q) = (\delta_{\mu\nu} - q_\mu q_\nu/q^2)/q^2$ in Landau gauge, $g^2_{\rm eff}$ is chosen to reproduce static and dynamic properties of hadrons below 1GeV and the interaction $\mathcal{G}(q^2)$ is modeled appropriately. For the sake of illustration, we select the well known Maris-Tandy model (MT) [28]

$$\begin{aligned} g^2_{\rm eff}\frac{\mathcal{G}(q^2)}{q^2} &= \frac{4\pi^2 D q^2 \exp\left(-\frac{q^2}{\omega^2}\right)}{\omega^6} \\ &+ \frac{8\pi^2\gamma_m\left(1-\exp\left(-\frac{q^2}{4m_t^2}\right)\right)}{q^2\log\left(\tau+(1+\frac{q^2}{\Lambda^2_{\rm QCD}})^2\right)} \ , \end{aligned} \tag{7}$$

where $m_t = 0.5$ GeV, $N_f = 4$, $\tau = e^2 - 1$, $D = (0.96\text{GeV})^2$, and $\omega = 0.4$ GeV. This model has extensively been used in SDE studies of hadron phenomenology. With a quark bare mass $m_b = 7$MeV, choosing the renormalization scale at $\zeta = 2$ GeV, the solution to the gap equation is depicted in Fig. 1. Some important remarks are:

The infrared enhancement of the mass function is the smoking gun for DCSB. It describes constituent quark masses with a value of 600 MeV [2], as expected for light-quark phenomenology. Non-perturbative effects dominate in the region $0 < p^2 < 1$ GeV^2. At higher energies, the mass function evolves smoothly toward the asymptotically free current quark mass. This is a long-standing prediction of SDEs studies.

[2] In the chiral limit is obtained a mass of 500MeV

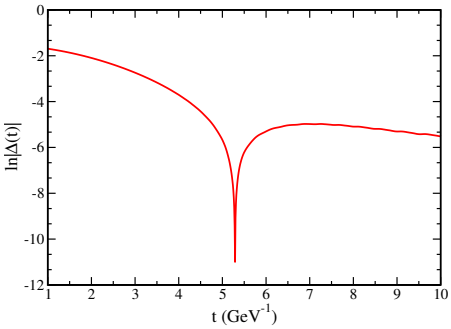

Fig. 2 Spatially averaged scalar quark propagator for the MT model, Eq. (7). Cusp indicates confinement.

Relevant hadron observables that can be obtained directly from the quark propagator are, for instance, the vacuum chiral condensate

$$-\langle\bar{\psi}\psi\rangle = \lim_{\Lambda\to\infty} Z_4 N_c \mathrm{Tr}_D \int^{\Lambda} \frac{d^4k}{(2\pi)^4} S(k) \\ \sim (0.27 \text{ GeV})^3 \,. \tag{8}$$

The trace in this expression is taken over Dirac indices in the chiral limit and $N_c = 3$. A second example is the pion leptonic decay constant, which can be calculated from the Pagel-Stokar equation [33]

$$f_\pi^2 = -\frac{N_c}{4\pi^2} \int^{\Lambda} dk^2 \frac{k^2 F(k^2)}{(k^2 + M^2(k^2))^2} \\ \times \left[M^2(k^2) - \frac{k^2}{2} M(k^2) \frac{dM(k^2)}{dk^2} \right] \\ \sim (0.09 \text{ GeV})^2. \tag{9}$$

Moreover, quark confinement is encoded in the quark propagator. We can observe it through the violation of the Osterwalder-Schrader axiom of reflexion positivity [34]. Let us define the scalar part of the spatially averaged propagator via the function [35, 36]

$$\Delta(t) = \int d^3x \int \frac{d^4p}{(2\pi)^4} e^{ip\cdot x} \sigma_s(p^2) \,. \tag{10}$$

In Fig. 2 we draw $\log|\Delta(t)|$. The cusp in this curve is related to a zero of $\Delta(t)$, which indicates a change of sign of this function and provides a clear, visual, definitive description of quark confinement. The inverse of the position of the cusp serves as an order parameter for confinement [36], and for this model, it corresponds, precisely, to the scale of the dynamically generated mass, namely, a few hundred MeV.

Below we propose alternative effective models for the gap equation in order to study their behavior and compare with the Maris-Tandy model. Our goal is to reproduce as closely as possible the features just described.

3 Dressed Gluon Propagators

We consider the following gluon dreesing functions:

$$\frac{\mathcal{G}_{\rm I}(q^2)}{q^2} = fz(\zeta)\frac{q^2+m_0^2}{q^4+q^2m_0^2+m_0^4}\,, \tag{11a}$$

$$\frac{\mathcal{G}_{\rm II}(q^2)}{q^2} = fz(\zeta)\,{\rm Sinc}^2(q)\,, \tag{11b}$$

$$\frac{\mathcal{G}_{\rm III}(q^2)}{q^2} = fz(\zeta)\frac{H_1(q)}{q^2}\,, \tag{11c}$$

$$\frac{\mathcal{G}_{\rm IV}(q^2)}{q^2} = fz(\zeta)\frac{2/\pi}{q^2+m_1^2}\,, \tag{11d}$$

where $f=-b\sqrt{2\pi}$. the factor $z(\zeta)$ is introduced such that at the renormalization point $\mathcal{G}_j(\zeta^2)=1$. We label the models for each j as follows: I (RGZ), II (Sinc), III (Struve) and IV (Struve Lineal).

In the above expressions, the RGZ Model (Equation (11a)) is a refined version which captures the scale of the transition of the $1/p^2$ behavior through the mass scale $m_0 = 2.167$GeV. This form advocates the non-perturbative, lattice inspired form of the gluon propagator proposed in [31]:

$$\frac{\mathcal{G}(q^2)}{q^2} = \frac{z(\zeta)(q^2+M^2)}{q^4+q^2M^2+M^4}. \tag{12}$$

were the non-perturbative scale is driven by $M = 0.5$ GeV. Again, the factor $z(\zeta)$ is introduced to entail the MOM renormalization condition $\mathcal{G}(\zeta^2)=1$ is satisfied.

The Sinc Model is motivated by a Fourier Transform of the Rosen-Morse trigonometric potencial used to describe a quark-diquark interaction [27]. The Struve Model is similar, but the instantaneous propagator has a different form obtained by projecting the hyperspherical motion onto the equatorial disk $\mathcal{D}_3$, a plane 3D space, and then performing a 3D Fourier transform to momentum space. [25]. The Struve Lineal model is a simplified version of the Struve dressing, which retains the infrared height and ultraviolet fall-off with the scale $m_1=\sqrt{3}$GeV.

All the gluon models presented in Equations (11) and (12) have some common properties: they are finite at low momentum and decrease as $1/q^2$ at high momentum. The oscillations that are visible in the Sinc dressing for momentum values between 1 GeV and 10 GeV (in the Struve dressing, these oscillations are less visible) can be explained by the finite volume of S^3 compared to the infinite volume of E_4. As a result, our model is reliable only up to a scale of 1 GeV, where it can describe a gluon that acquires a dynamically generated mass. For momentum values greater than 1 GeV,

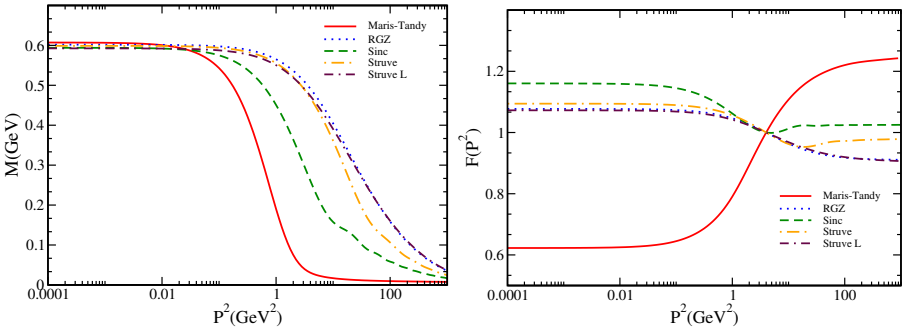

Fig. 3 Quark propagator with the effective gluon dressing function in Eq. (11) reproducing the constituent quark masses of the MT model. *Left panel:* Mass Function. *Right panel:* Wave function renormalization for different models.

Model	$M(0)$ [GeV]	-$\langle\psi\psi\rangle$ [GeV^3]	f_π [GeV]
MT	0.6	$(0.506)^3$	0.108
RGZ	0.6	$(0.451)^3$	0.270
Sinc	0.6	$(0.413)^3$	0.195
Struve	0.6	$(0.403)^3$	0.254
Struve Lineal	0.6	$(0.460)^3$	0.265

Table 1 Observables computed with the effective model contrasted against the MT predictions fitting to the height of the mass function.

the constant f is replaced by a momentum-dependent function $f(q^2)$,

$$f\left(q^2\right) \simeq \frac{\pi\gamma}{\ln\left(e + \frac{q^2}{\Lambda_{\rm QCD}^2}\right)}\,, \tag{13}$$

which smoothly drives the quark propagator towards its perturbative behavior. The weaker enhancement of the mass function in the infrared in our models compared to the lattice-inspired model in Equation (12) may be due to the choice of parameters used to fit the unflavored meson spectra. Further work is needed to select an appropriate value of $g^2_{\rm eff}$ for static and dynamic hadron phenomenology.

To start, we choose $g^2_{\rm eff}$ in the gap equation so that the height of the quark mass function is similar to that of the MT model. Figure 3 shows the propagator for various models. The effective dressing of the gluon leads to a non-perturbative enhancement of the mass function at low momentum, which transitions to the expected behavior in the domain of asymptotic freedom. The mass function for the effective models is wider than that of the MT model, as neglecting vertex dressing causes broadening due to the large support of the gluon propagator. This broadening results in a slight underestimation of the values of the chiral condensate $-\langle\bar{\psi}\psi\rangle$ and f_π, as shown in Table 1. The non-perturbative effects of the gluon dressing also impact the confinement test on the dynamically generated quark propagator shown in Fig. 4, as the late appearance of the cusp indicates that the confinement scale is slightly smaller in this case but still in the same order as in the MT case.

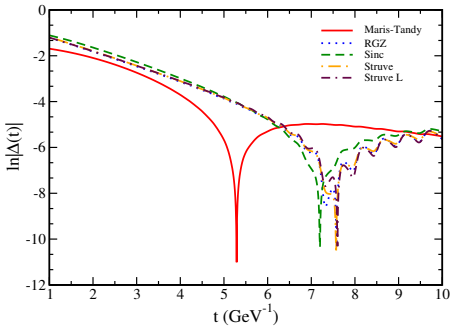

Fig. 4 Confinement test for the model fitting the constituent quark mass.

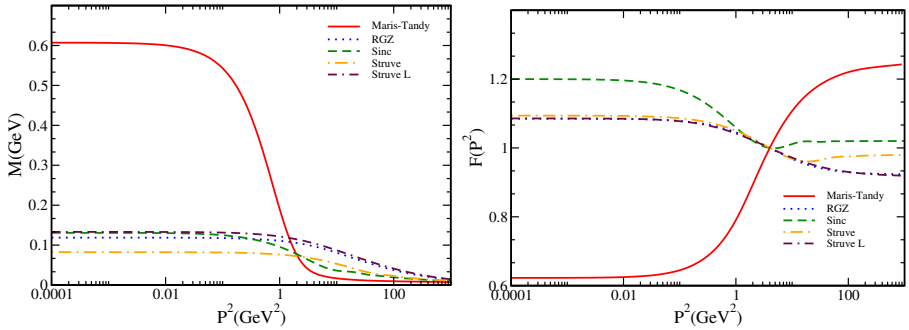

Fig. 5 Quark propagator reproducing the chiral condensate, using Eqs. (11). *Left panel:* Mass Function. *Right panel:* Wave function renormalization for different models.

Model	$M(0)$ [GeV]	-$\langle\psi\psi\rangle$ [GeV^3]	f_π [GeV]
MT	0.6	$(0.506)^3$	0.108
RGZ	0.12	$(0.505)^3$	0.079
Sinc	0.13	$(0.509)^3$	0.071
Struve	0.081	$(0.501)^3$	0.057
Struve Lineal	0.13	$(0.506)^3$	0.085

Table 2 Observables computed with the effective model contrasted against the MT predictions fitting to the condensate.

Considering that the chiral condensate is the quantity that can be experimentally measured and has an impact on hadron phenomenology rather than the quark constituent mass, we proceeded to adjust the value of $g^2_{\rm eff}$ such that it matches the chiral condensate of the MT model. The obtained results are illustrated in Fig. 5. The growth of the mass function at low energies is reduced significantly, resulting in weaker non-perturbative effects. This decrease is evident from the smaller predicted value of f_π and the confinement test presented in Fig. 6, as the cusp in the confinement test appears much later.

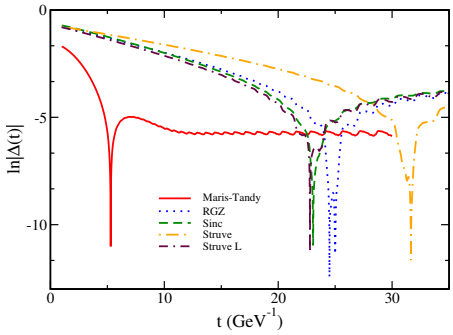

Fig. 6 Confinement test for the model fitting the chiral condensate.

4 Summary and discussion

In this work, we adopt four different dressed gluon propagator models and use in the kernel of the SDEs and compare the computed results with those obtained with the Maris-Tandy model. With those dressing functions, we study DCSB and confinement by means of the SDE for the quark propagator. We observe a dynamical enhancement of the mass function $M(p^2)$ in the infrared driven by the effective gluon propagator, which also provides the expected $1/p^2$ attainable fall-off of this function in the perturbative domain. However, for all models, this fall-off comes later than with the Maris-Tandy model.

Instead of using a quark in the chiral limit, we adopted a quark bare mass $m_b = 7$MeV and a renormalization scale at $\zeta = 2$ GeV, and we obtained a dressed quark mass of 600MeV. As a result, when we adjusted the constant f in the four models of Eq. (11) to match the quark-dressed mass of the MT model, we obtained a condensate that it does not match with the condensate in the chiral limit. This result can be explained by considering that the dressed mass depends on the renormalization point. However, a renormalization point invariant condensate can be defined [16] to have a gauge invariance model.

The effects of unfolding the finite volume into an infinite space do not modify the asymptotics of $M(p^2)$. All the tested propagators violate the axiom of reflexion positivity, indicating that the same effective gluon dressing is responsible for quark confinement in our model. However, those models still need an improvement to achieve a full agreement for the predictions of the chiral condensate, pion decay constant and quark constituent mass. We hope that considering static and dynamical properties of hadrons could be included in the models to obtain a light meson spectra with appropriate selection of the potential parameters. This open an opportunity to develop extensions of the present work.

Acknowledgments. We acknowledge enlightening discussions from M. Kirchbach and the organizers of Baryons 2022 for the excellent organization.

References

[1] S. J. Brodsky, V. D. Burkert, D. S. Carman, J. P. Chen, Z. F. Cui, M. Döring, H. G. Dosch, J. Draayer, L. Elouadrhiri and D. I. Glazier, *et al.* Int. J. Mod. Phys. E **29**, no.08, 2030006 (2020) doi:10.1142/S0218301320300064

[2] C. D. Roberts and A. G. Williams, Prog. Part. Nucl. Phys. **33**, 477 (1994).

[3] C. D. Roberts and S. M. Schmidt, Prog. Part. Nucl. Phys. **45**, S1 (2000).

[4] P. Maris and C. D. Roberts, Int. J. Mod. Phys. E **12**, 297 (2003).

[5] M. R. Pennington, J. Phys. Conf. Ser. **18**, 1 (2005).

[6] A. Höll, C. D. Roberts and S. V. Wright, (nucl-th/0601071).

[7] C. S. Fischer, J. Phys. G **32**, R253 (2006).

[8] C. D. Roberts, M. S. Bhagwat, A. Höll and S. V.Wright, Eur. Phys. J. ST **140**, 53 (2007).

[9] C. D. Roberts, Prog. Part. Nucl. Phys. **61**, 50 (2008).

[10] R. J. Holt and C. D. Roberts, Rev. Mod. Phys. **82**, 2991 (2010).

[11] L. Chang and C. D. Roberts, AIP Conf. Proc. **1361**, 91 (2011).

[12] E. S. Swanson, AIP Conf. Proc. **1296**, 75 (2010).

[13] L. Chang, C. D. Roberts and P. C. Tandy, Chin. J. Phys. **49**, 955 (2011).

[14] P. Boucaud et al., Few Body Syst. 53 (2012) 387-436.

[15] A. Bashir, L. Chang, I. C. Clöet, B. El-Bennich, Y.-X. Liu, C. D. Roberts, and P. C. Tandy, Commun. Theor. Phys. 58, 79 (2012).

[16] M. A. Sultan, F. Akram, B. Masud and K. Raya, Phys. Rev. D **103**, no.5, 054036 (2021).

[17] L. Chang, Y. B. Liu, K. Raya, J. Rodríguez-Quintero and Y. B. Yang, Phys. Rev. D **104**, no.9, 094509 (2021).

[18] A. Deur, V. Burker, J. P. Chen, and W. Korsch, Phys. Lett. **665**, 349 (2008).

[19] J. Maldacena, Phys. Rev. Lett. **80**, 4859 (1998).

[20] Witten E 1998, *Adv. Theor. Math. Phys.* **2**, 233.

[21] Hands S, Hollowood T J and Myers J C 2010, *JHEP* **1007** 086.

[22] M. Kirchbach, A. Pallares-Rivera, C. Compean, and A. Raya, J. Phys. Conf. Ser. **378**, 012036 (2012) doi:10.1088/1742-6596/378/1/012036.

[23] A. Pallares-Rivera and M. Kirchbach, J. Phys. A:Math.Theor. **44**, 44530 (2011).

[24] C.B. Compean and M. Kirchbach, J. Phys. A: Math. Theor. **42** 365301 (2009).

[25] C. B. Compean, M. Kirchbach, J. Phys. A:Math.Theor. **44**, 015304 (2011).

[26] C. Rasinariu, J. V. Mallow, and A. Gangopadhyaya, C. Eur. J. Phys. **5**, 111 (2007).

[27] C. B. Compean and M. Kirchbach, Eur. Phys. J. A **33**, 1 (2007).

[28] P. Maris and P. C. Tandy, *Phys. Rev. C***60** 055214 (1999).

[29] S. x. Qin, L. Chang, Y. x. Liu, C. D. Roberts and D. J. Wilson, Phys. Rev. C **84**, 042202 (2011) doi:10.1103/PhysRevC.84.042202.

[30] D. Dudal, J. A. Gracey, S. P. Sorella, N. Vandersickel and H. Verschelde, Phys. Rev. D **78**, 065047 (2008) doi:10.1103/PhysRevD.78.065047.

[31] A. Ayala, A. Bashir, D. Binosi, M. Cristoforetti and J. Rodriguez-Quintero, Phys. Rev. D 86, 074512(2012).

[32] M. S. Bhagwat, I. C. Clöet and C. D. Roberts, (arXiv:0710.2059 [nucl-th]), in *Proceedings of the Workshop on Exclusive Reactions at High Momentum Transfer,* Newport News, Virginia, 21-24 May 2007, Eds. A. Radyushkin and P. Stoler (World Scientific, Singapore, 2007).

[33] J.C. Taylor, Nucl. Phys. **B**33, 436 (1971).

[34] K. Osterwalder and R. Schrader, Commun. Math. Phys. **31**, 83 (1973); *ibid*, Commun. Math. Phys. 42, 281 (1975).

[35] L. C. L. Hollenberg, C. D. Roberts, and B. H. J. McKellar, Phys. Rev. C **46**, 2057 (1992); F. T. Hawes, C. D. Roberts, and A. G.Williams, Phys. Rev. D **49**, 4683 (1994)

[36] A. Bashir and A. Raya, Nucl. Phys. B **709**, 307 (2005); A. Bashir and A. Raya, Few-Body Syst. **41**, 185 (2007); C. P. Hofmann, A. Raya, and S. Sanchez Madrigal, Phys. Rev. D **82**, 096011 (2010).

[37] M. P. Dabrowski, J. Garecki, and D. B. Blaschke, Ann. Phys. (Leipzig) **18**, 13 (2009).